



Original article

Nitric oxide donating anilinopyrimidines: Synthesis and biological evaluation as EGFR inhibitors



Chun Han^{a,b,1}, Zhangjian Huang^{a,b,1}, Chao Zheng^c, Ledong Wan^{a,b}, Yisheng Lai^{a,b}, Sixun Peng^{a,b}, Ke Ding^{d,**}, Hongbin Ji^{c,***}, Yihua Zhang^{a,b,*}

^aState Key Laboratory of Natural Medicines, China Pharmaceutical University, Nanjing 210009, PR China

^bCenter of Drug Discovery, China Pharmaceutical University, Nanjing 210009, PR China

^cState Key Laboratory of Cell Biology, Institute of Biochemistry and Cell Biology, Shanghai Institutes for Biological Sciences, Chinese Academy of Sciences, Shanghai 200030, PR China

^dKey Laboratory of Regenerative Biology and Institute of Chemical Biology, Guangzhou Institutes of Biomedicine and Health, Chinese Academy of Sciences, Guangzhou 510530, PR China

ARTICLE INFO

Article history:

Received 12 March 2013

Received in revised form

18 May 2013

Accepted 20 May 2013

Available online 29 May 2013

Keywords:

Nitric oxide

EGFR inhibitor

Anilinopyrimidine

Antiproliferative activity

WZ4002

ABSTRACT

To search for potent nitric oxide (NO) donating epidermal growth factor receptor (EGFR) inhibitors, a series of phenylsulfonylfuroxan-based anilinopyrimidines **10a–h** were synthesized and biologically evaluated. Compounds **10f–h** exhibited potent inhibitory activity against EGFR L858R/T790M and were as potent as WZ4002 in inhibition of H1975 cells harboring EGFR L858R/T790M. Additionally, **10h** produced high levels of NO in H1975 cells but not in normal human cells, and its antiproliferative activity was diminished by hemoglobin, an NO scavenger. Furthermore, **10h** inhibited EGFR activation and downstream signaling in H1975 cells. These results suggest that the strong antiproliferative activity of **10h** could be attributed to the synergic effects of high levels of NO production and inhibition of EGFR and downstream signaling in the cancer cells.

© 2013 Elsevier Masson SAS. All rights reserved.

1. Introduction

Non-small cell lung cancer (NSCLC) is the leading cause of cancer-related death worldwide, and only less than 15% of NSCLC patients are anticipated to be alive for five years after diagnosis [1,2]. Currently, one of the most important therapeutic targets for NSCLC is epidermal growth factor receptor (EGFR) tyrosine kinase [3]. EGFR is essential for cell proliferation, survival, adhesion, migration, and differentiation through activation of downstream signaling pathway [4]. Deregulation of EGFR signaling attributed to overexpression or constitutive activation can promote malignant transformation, and is correlated with poor prognosis in NSCLC [5].

The first generation ATP-competitive and reversible EGFR inhibitors such as gefitinib and erlotinib (Fig. 1) are effective for patients harboring a short in-frame deletion of exon 19 (del E746_A750) and the L858R point mutation in exon 21 in the EGFR domain [6]. Unfortunately, the secondary mutation in the catalytic domain of EGFR exon 20 (T790M) causes about 50% of NSCLC cases to develop resistance after repeated treatments by the first generation EGFR inhibitors [7,8]. EGFR T790M mutation restores the affinity for ATP similar to that of wild type (WT) EGFR, and prevents the reversible inhibitors from binding at higher ATP concentrations [9].

The irreversible EGFR inhibitors, as the second generation inhibitors, including CI-1033 [10], BIBW2992 [11], HKI-272 [12], PF00299804 [13] (Fig. 1) have been shown to be superior to the reversible peers against EGFR T790M [14]. These inhibitors are structurally characterized by a quinazoline-type scaffold connecting an electrophilic functionality (acrylamide or analogous moiety) that can undergo a Michael addition reaction with a conserved cysteine residue Cys797 present in EGFR to achieve greater occupancy than the reversible inhibitors [15]. Therefore, the irreversible EGFR inhibitors can circumvent competition with ATP to overcome the T790M mutation related resistance [16]. Nevertheless, since

* Corresponding author. Center of Drug Discovery, China Pharmaceutical University, Nanjing 210009, PR China. Tel./fax: +86 25 83271015.

** Corresponding author. Tel.: +86 20 32015276; fax: +86 20 32015299.

*** Corresponding author. Tel.: +86 21 54921108; fax: +86 21 54921101.

E-mail addresses: ding_ke@gibh.ac.cn (K. Ding), hbj@sibs.ac.cn (H. Ji), zyhtgd@163.com, zyhtgd@hotmail.com (Y. Zhang).

¹ These two authors contributed equally to this work.

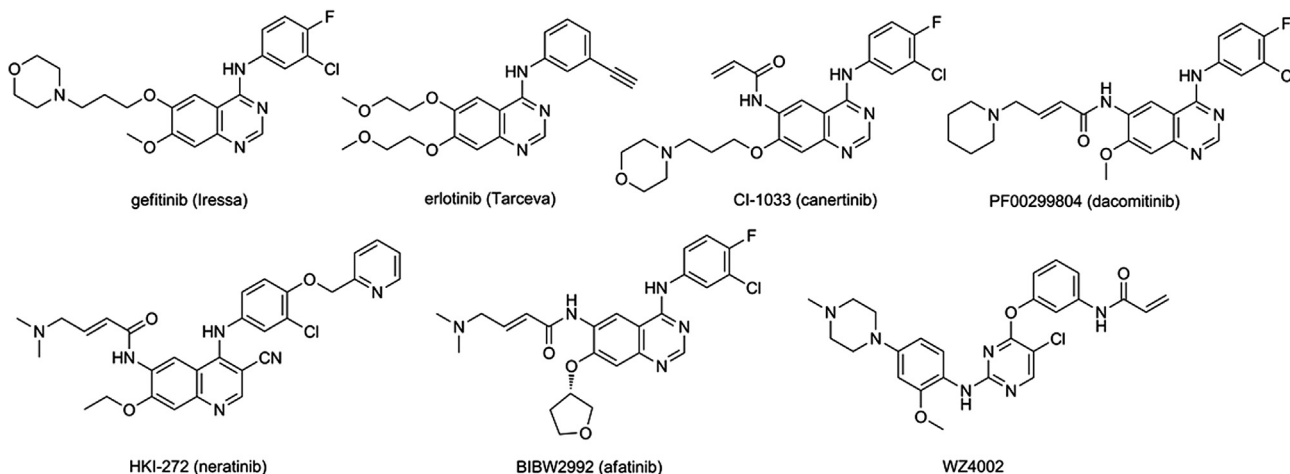


Fig. 1. Chemical structures of reversible and irreversible EGFR inhibitors.

EGFR T790M and WT EGFR exhibit a similar affinity to ATP [9], the quinazoline-based EGFR inhibitors could inhibit both EGFR T790M and WT EGFR at the same concentration. Therefore, the clinical efficacy of these inhibitors has been limited, especially in patients with gefitinib- or erlotinib-resistant NSCLC, by some side effects such as the dose-limiting toxicity, diarrhea and skin rash [17].

Recently, novel irreversible EGFR inhibitors with an anilino-pyrimidine scaffold were reported by Gray et al. [18]. These inhibitors can display good selectivity against EGFR T790M mutant over WT EGFR, exemplified by WZ4002 [19] (Fig. 1), which exhibits 30–100-fold stronger inhibitory activity against EGFR T790M, but 100-fold less inhibitory activity against WT EGFR as compared with the irreversible quinazoline-based inhibitors in vitro. Accordingly, the anilino-pyrimidine is supposed to be an attracting scaffold for the design of small molecule inhibitors against EGFR T790M.

Nitric oxide (NO), a signaling and effector molecule, plays a pivotal role in diverse physiological and pathophysiological processes [20]. It is generally believed that high levels of NO generated from NO-donors can not only induce apoptosis and inhibit metastasis of tumor cells, but also sensitize tumor cells to chemotherapy, radiation and immunotherapy in vitro and in vivo [21]. In this regard, the combination of NO with anti-cancer agents could increase the therapeutic efficacy and retard the development of drug resistance [22]. Furoxan, an important class of NO donors, is able to produce high levels of NO in vitro and inhibit the growth of tumors in vivo [23]. Our group has developed a variety of phenylsulfonylfuroxan-based NO releasing compounds that exhibited potent and selective antitumor activity in vitro and in vivo [24–26].

It is therefore of interest to investigate whether introduction of phenylsulfonylfuroxan moiety to the anilino-pyrimidine scaffold would provide a hitherto unknown class of NO donating EGFR inhibitors that may release high levels of NO to exert synergistic antitumor effects with anilino-pyrimidines. As part of our ongoing research program, a series of phenylsulfonylfuroxan-based anilino-pyrimidines **10a–h** were synthesized, and their EGFR kinase inhibitory activity, antiproliferation against several NSCLC cell lines, in vitro NO release, and effects on EGFR and downstream signaling were biologically evaluated.

2. Chemistry

Compounds **10a–h** were synthesized as depicted in Scheme 1. Substituted phenol **4a** was prepared from hydroxycinnamic acid **1** by esterification and subsequent hydrogenation [27] while phenols **4b–d** were commercially available. The phenols

4a–d were regioselectively coupled to the 4-position of 2,4,5-trichloropyrimidine to afford aryl ethers **5a–d**. On the other hand, cyclic amines **6a–c** were treated with 5-fluoro-2-nitrophenyl methyl ether to furnish nitro arylamines **7a–c**, which underwent reduction to generate corresponding arylamines **8a–c**. Coupling of **5a–d** with **8a–c** in the presence of trifluoroacetic acid under reflux offered anilino-pyrimidines **9a–h**, which were condensed with diphenylsulfonylfuroxan **11** prepared via a three-step reaction sequence as described previously [24] to provide mono-phenylsulfonylfuroxans **10a–h**.

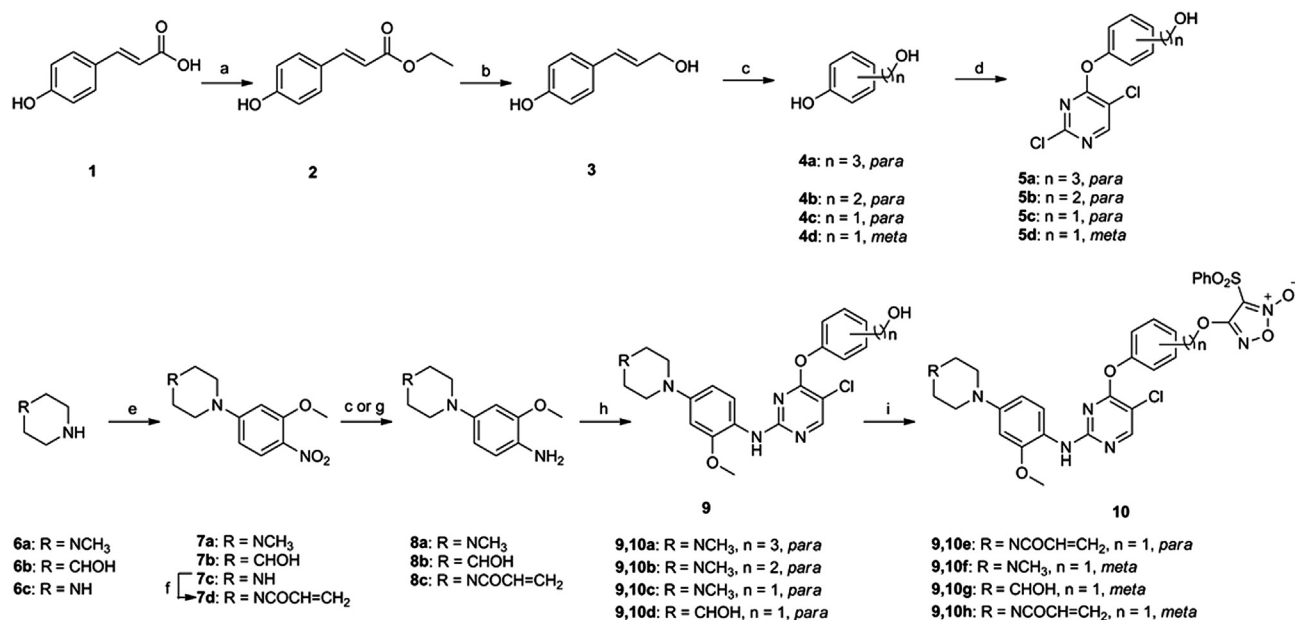
3. Results and discussion

3.1. Kinase inhibitory activity

The inhibitory activities of the target compounds **10a–h** against different types of kinases (EGFR WT, EGFR L858R, EGFR L858R/T790M) were evaluated using a well-established FRET-based Z'-Lyte assay [28,29], and gefitinib and WZ4002 were employed as positive controls. As shown in Table 1, all of the tested compounds exhibited high selective and strong inhibitory activity against EGFR L858R/T790M over WT EGFR and EGFR L858R as WZ4002 did. However, the ability of all compounds to inhibit EGFR L858R/T790M was lower than WZ4002 but superior to gefitinib. Generally, the compounds with *meta*-furoxan substitution on the benzene ring displayed stronger inhibitory activity on EGFR L858R/T790M than *para*-ones. For instance, compounds **10f–h** (IC_{50} = 0.019, 0.068, and 0.045 μ M, respectively) were more active than compounds **10a–e** (IC_{50} = 0.14–0.96 μ M) in inhibition of EGFR L858R/T790M.

3.2. Inhibitory activity on gefitinib-resistant H1975 and -sensitive HCC827 cells

The antiproliferative effects of the target compounds **10a–h** on NSCLC cell lines gefitinib-resistant H1975 (harboring EGFR L858R/T790M) and gefitinib-sensitive HCC827 (bearing EGFR del E746_A750) were investigated with gefitinib and WZ4002 as controls by an MTT assay. As can be seen in Table 2, consistent with their kinase inhibition, most of these compounds displayed higher antiproliferative activity on H1975 cells (IC_{50} = 0.052–0.372 μ M) than gefitinib (IC_{50} = 8.589 μ M). Notably, compounds **10f–h** (IC_{50} = 0.052–0.068 μ M) with the furoxan moiety linked to the *meta*-position of phenyl ring were as potent as WZ4002 (IC_{50} = 0.064 μ M), and showed stronger inhibitory activity against H1975 cells than *para*-substituted



Scheme 1. Synthesis of the target compounds **10a–h**. Reagents and conditions: (a) EtOH, H₂SO₄, reflux, 4 h; (b) LiAlH₄, BnCl, dry THF, rt, 4 h; (c) H₂, Pd/C, MeOH, rt, overnight, (for **4a**, **8a** and **8b**); (d) 2,4,5-trichloropyrimidine, K₂CO₃, DMF, rt, 2 h; (e) 5-fluoro-2-nitrophenyl methyl ether, K₂CO₃, DMSO, rt, overnight (for **7a** and **7b**); dioxane, 120 °C, 2 h (for **7c**); (f) acrylic acid, DCC/DMAP, anhydrous CH₂Cl₂, rt, overnight; (g) iron powder, NH₄Cl, THF/H₂O (1/1, v/v), reflux, 3 h, (for **8c**); (h) **5a–d**, TFA, 2-BuOH, reflux, 3 h; (i) 3,4-bis(phenylsulfonyl)-1,2,5-oxadiazole-2-oxide (**11**), NaH, anhydrous THF, rt, 0.5 h.

analogs **10a–e** (IC₅₀s = 0.148–0.372 μM). Additionally, **10f–h** were also active against HCC827 cells (IC₅₀s = 0.022–0.063 μM).

3.3. Activity on the cell lines harboring WT EGFR

As shown in Table 1, the target compounds did not significantly suppress WT EGFR relative to EGFR L858R/T790M. To validate that, the antiproliferative activity of the target compounds against cell lines harboring WT EGFR were investigated. The tested cell lines included NSCLC cells A549 possessing WT EGFR and *k-Ras* mutation-activating bypass MAPK signal pathway, human epithelial carcinoma cells A431 which overexpress WT EGFR, and human normal bronchial epithelial cell line 16HBE harboring WT EGFR. It can be seen from Table 2, most of compounds showed lower to moderate inhibitory activity against the cell lines harboring WT EGFR, comparable or superior to WZ4002. The compounds **10f–h** exhibited less antiproliferative activity on A549 cells (IC₅₀ = 4.189, 3.905 and 1.715 μM, respectively) and A431 cells (IC₅₀ = 1.356, 1.201 and 0.348 μM, respectively) relative to their inhibition against H1975 and HCC827 cells, suggesting that these compounds might

Table 1
Inhibitory activity of compounds **10a–h** against different types of EGFRs in vitro.

Compound	EGFR IC ₅₀ (μM) ^a		
	WT	L858R	L858R/T790M
10a	2.28	>10	0.78
10b	2.94	5.36	0.96
10c	1.09	1.53	0.14
10d	3.15	3.22	0.25
10e	>10	>10	0.41
10f	0.13	0.15	0.019
10g	0.24	0.49	0.068
10h	0.35	0.37	0.045
Gefitinib	0.0001	0.0002	0.941
WZ4002	0.0032	0.0054	0.0008

^a EGFR activity assays were performed using the FRET-based Z'-Lyte assay according to the manufacturer's instructions. The compounds were incubated with the kinase reaction mixture for 1.5 h before measurement. The data were means of three independent experiments.

possess a good selectivity against NSCLC cells with EGFR mutants over the other cancer cells. Additionally, **10f–h** showed much less inhibition on the growth of 16HBE cells (IC₅₀ = 2.207, 3.251 and 1.928 μM, respectively), which was approximately 35–50 fold less potent than their inhibition against the H1975 and HCC827 cells, suggesting the safety profile of these compounds.

3.4. Effects of NO on antiproliferative activity

3.4.1. The antiproliferative activity was positively correlated with NO release

Next, the effects of NO on the antiproliferative activity of target compounds against NSCLC cells were evaluated. In this regard, NSCLC cells H1975 and normal human bronchial epithelial cells 16HBE were respectively exposed to compounds **10a**, **10b**, **10g**, **10h**,

Table 2
Antiproliferative activities of compounds **10a–h** against cells harboring a different status of EGFR.

Compound	IC ₅₀ (μM) ^a				
	H1975 ^b	HCC827 ^c	A549 ^d	A431 ^e	16HBE ^f
10a	0.315	4.817	2.835	0.551	3.519
10b	0.372	1.928	3.746	0.479	2.423
10c	0.221	0.863	3.655	2.199	2.296
10d	0.148	0.095	4.254	0.357	2.192
10e	0.154	4.902	3.902	4.659	3.371
10f	0.052	0.063	4.189	1.356	2.207
10g	0.068	0.036	3.905	1.201	3.251
10h	0.055	0.022	1.715	0.348	1.928
Gefitinib	8.589	0.006	4.626	8.982	1.601
WZ4002	0.064	0.009	3.354	1.115	0.811

^a The inhibitory effects of individual compounds on the proliferation of cancer cell lines were determined by the MTT assay. The data were means from at least three independent experiments.

^b H1975 is a human lung cancer cell line (EGFR L858R/T790M).

^c HCC827 is a human lung cancer cell line (EGFR del E746_A750).

^d A549 is a human lung cancer cell line (WT EGFR/*k-Ras* dependent).

^e A431 is human epithelial carcinoma cell line (overexpressed WT EGFR).

^f 16HBE is a normal human bronchial epithelial cell line.

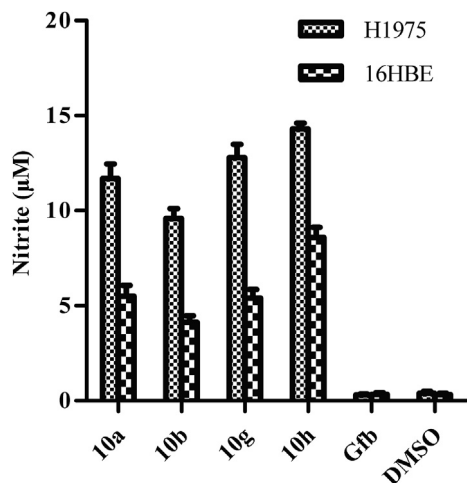


Fig. 2. Variable levels of NO (presented as nitrite) produced by the indicated compounds. H1975 and 16HBE cell lines were treated with individual compounds at 100 μM for 150 min, and the contents of nitrite in the cell lysates were determined by Griess assay. The individual values were determined by measuring absorbance at 540 nm and calculated according to the standard curve. Data shown were the mean values \pm SEM of each compound in individual types of cells from three experiments. Gfb: gefitinib.

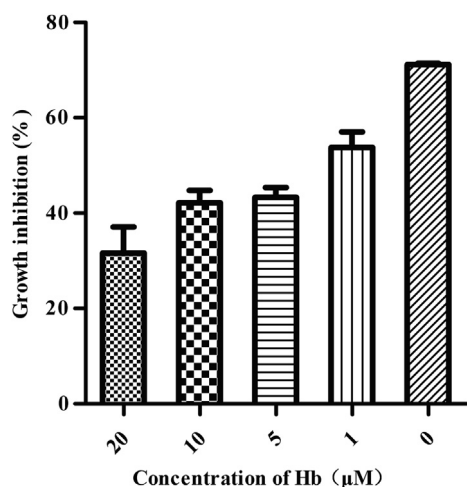


Fig. 3. NO produced by **10h** contributed to the inhibitory effect on cell proliferation. H1975 cells were pretreated with the indicated concentrations of hemoglobin (Hb) (0, 1, 5, 10 or 20 μM) for 1 h and treated with 1 μM of **10h** for 24 h. The results were expressed as percent of cell growth inhibition relative to control cells. Data were mean values \pm SEM obtained from three independent experiments.

gefitinib (each at 100 μM) and DMSO for the same incubation time. The levels of NO generated in the cell lysates were determined and presented as that of nitrite (Fig. 2) using a Griess assay [30]. As expected, treatment with gefitinib or DMSO resulted in little nitrite in both H1975 and 16HBE cells. In contrast, treatment with the

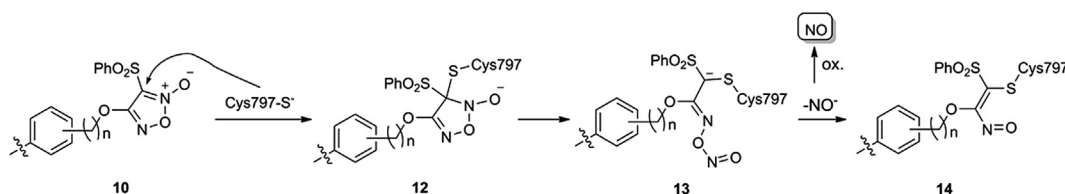
tested compounds generated variable levels of nitrite in H1975 cells. Interestingly, treatment with less active compounds **10a** and **10b** produced lower levels of nitrite, whereas more active compounds such as **10g** and **10h** produced higher levels of nitrite in these cells, indicating that the amounts of NO released by these compounds were positively correlated with their inhibitions on H1975 cells in vitro ($R = 0.907$, $p < 0.05$, determined by Pearson's correlation analysis). Additionally, the levels of nitrite produced by **10g** and **10h** in 16HBE cells were much less than that in H1975 cells. These results suggest that the target compounds may selectively produce high levels of NO in NSCLC cells with EGFR mutations but not in normal human cells harboring WT EGFR, which is in agreement with their strong selective inhibition on proliferation of NSCLC cells with EGFR mutations in vitro.

3.4.2. The antiproliferative activity was diminished by an NO scavenger

To verify the contribution of NO to the inhibitory activity, **10h** was selected to test its antiproliferative effects in the presence or absence of an NO scavenger, hemoglobin. H1975 cells were pre-treated with various concentrations of hemoglobin for 1 h and then treated with 1 μM of **10h**. The effects of different treatments on the growth of H1975 cells were determined by the MTT assay (Fig. 3). It was observed that treatment with **10h** alone significantly inhibited the growth of H1975 cells and this inhibitory effect was dramatically reduced by pretreatment with hemoglobin in a dose-dependent manner. These results clearly demonstrate that NO production by the compound substantially contribute to its inhibition on NSCLC cell proliferation in vitro.

3.4.3. The mechanism of NO release

As reported previously [31,32], the sulfhydryl groups can induce the generation of NO from furoxans, we postulate that the phenylsulfonylfuroxan moiety of the target compounds is likely to release NO by the assistance of the conserved cysteine residue Cys797 on EGFR T790M. As shown in Scheme 2, a nucleophilic attack of Cys797-S⁻ on position 3 of the furoxan ring of **10** may lead to generation of the adduct **12**. Subsequently, ring opening of furoxan occurs to form the nitroso derivative **13**, which further eliminates nitrosyl anions (NO⁻) and produces nitroso compound **14**. Meanwhile, the eliminated nitrosyl anions furnish NO after oxidation. According to this assumption, the furoxan moiety of **10h** might bind with Cys797, as WZ4002 does, because **10h** and WZ4002 have a similar configuration at the Michael addition site, while the acrylamide group located at the piperazine moiety might be too far away from the Cys797 to bind. Furthermore, there was no significant difference in the potency for **10h**, **10f** and **10g** in kinase and cellular experiments, suggesting that the acrylamide may not be determinant factor for activity. Additionally, **10h** released higher levels of NO in H1975 cells than **10g** without an acrylamide group. These results suggest that the acrylamide group of **10h** might not reduce the efficiency of Cys797 in interacting with the furoxan group and subsequently not affect the amount of NO release.



Scheme 2. The speculative mechanism by which compounds **10a–h** may bind with Cys797 on EGFR T790M to release NO.

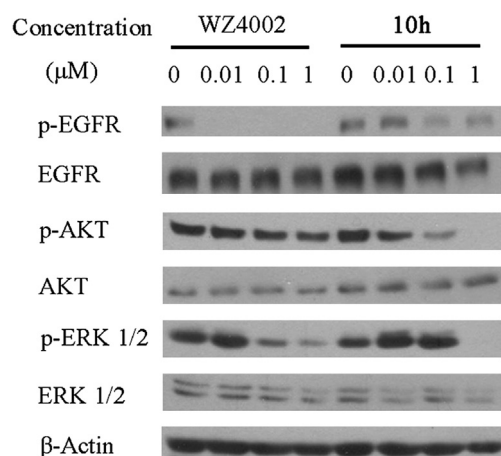


Fig. 4. Compounds **10h** and WZ4002 inhibited the activation of EGFR and downstream signaling in H1975 NSCLC cells harboring EGFR L858R/T790M.

3.5. Effects on EGFR activation and downstream signaling

In order to get insight into the mechanisms underlying the activity of these NO-releasing EGFR inhibitors, we subsequently examined the inhibitory effects of the active compound **10h** on the EGFR activation and downstream signaling in H1975 cells. The cells were treated with various concentrations of **10h** or WZ4002. The expression and activation of EGFR-related signal events, AKT and ERK were determined by immunoblotting, and the results were summarized in Fig. 4. It was observed that treatment with **10h** significantly inhibited the phosphorylation of EGFR in a dose-dependent manner but was less potent than WZ4002. However, the treatment by **10h** at 1 μM completely restrained the expression of downstream proteins p-Akt and p-Erk, which was slightly superior to WZ4002.

4. Conclusions

In summary, a series of phenylsulfonyluroxan-based anilino-pyrimidines **10a–h** were synthesized and biologically evaluated. Most of the compounds were more potent than gefitinib, especially **10f–h** showed stronger and selective inhibitory effects toward EGFR mutant L858R/T790M. These compounds also showed better inhibitory activity against H1975 cell line harboring EGFR L858R/T790M than gefitinib, among them, compounds **10f–h** were as potent as WZ4002 in inhibition of H1975 cell line. Furthermore, **10f–h** were also the most active compounds against gefitinib-sensitive HCC827 bearing EGFR del E746_A750. Importantly, these compounds only showed lower to moderate inhibition on the cells with WT EGFR (A431, A549 and 16HBE cells), suggesting that they might possess good selectivity and safety profiles. Interestingly, compound **10h** released much higher levels of NO in H1975 cells than in 16HBE cells, and the antiproliferative activity of **10h** in H1975 was diminished by an NO scavenger in a dose-dependent manner, suggesting that NO released by this compound may play an important role in antiproliferation of H1975 cells. Furthermore, the EGFR kinase inhibitory and antiproliferative activities of **10h** were further rationalized by Western blot analysis for activation of EGFR and the downstream signaling in H1975 cells. All these results suggest that the good antiproliferative activity of **10h** could be attributed to the synergic effect of high levels of NO production and inhibition of EGFR and related signaling in the cancer cells. Therefore, our novel findings provide a proof of principle in design of new NO-releasing EGFR inhibitors for the intervention of NSCLC.

We are interested in further investigation on the in vivo anti-NSCLC effects and the mechanisms underlying the action of **10h** in inhibition of human tumorigenesis of NSCLC.

5. Experimental protocols

5.1. Chemical analysis

Melting points of individual compounds were determined on a Mel-TEMP II melting point apparatus and uncorrected. ^1H NMR and ^{13}C spectra were recorded with a Bruker Avance 300 or 500 MHz spectrometer at 303 K, using TMS as an internal standard. MS spectra were recorded on a Mariner Mass Spectrum (ESI) and HRMS on Agilent technologies LC/MSD TOF. All compounds were routinely checked by TLC and ^1H NMR. TLCs and preparative TLCs were performed on silica gel GF/UV 254, and the chromatograms were conducted on silica gel (200–300 mesh) and visualized under UV light at 254 and 365 nm. All solvents were reagent grade and, when necessary, were purified and dried by standard methods. Solutions after reactions and extractions were concentrated using a rotary evaporator operating at a reduced pressure of ca. 20 Torr. Compounds **4b–d** were commercially available. **7a** [33], **7b** [34], **7c** [34], **8a** [33] and **8b** [35] were synthesized according to corresponding references and 3,4-bis(phenylsulfonyl)-1,2,5-oxadiazole-2-oxide (**11**) was synthesized as previously described [24].

5.1.1. 4-(3-Hydroxypropyl)phenol (**4a**)

Compound **3** [27] (1 g, 6.7 mmol) was stirred under H_2 in the presence of 10% palladium carbon (catalytic amount) in MeOH for 12 h. The mixture was filtered through a pad of Celite[®], the filtrate was dried and concentrated to offer **4a** as a white solid (0.99 g, 98% yield, m.p. 52–53 $^\circ\text{C}$); Analytical data for **4a**: ^1H NMR (500 MHz, CDCl_3): δ 1.83–1.89 (m, 2H), 2.63 (t, $J = 7.8$ Hz, 2H), 3.01 (brs, 1H), 3.67 (t, $J = 6.5$ Hz, 2H), 6.74 (d, $J = 8.4$ Hz, 2H), 7.05 (d, $J = 8.3$ Hz, 2H); ^{13}C NMR (75 MHz, CDCl_3): δ 155.68, 136.7, 129.94, 111.37, 62.06, 33.87, 31.48; ESI-MS: m/z 151.1 $[\text{M} - \text{H}]^-$; ESI-HRMS (m/z): $[\text{M} - \text{H}]^-$ calcd for $\text{C}_9\text{H}_{12}\text{O}_2$ 151.0765; obsd 151.0766.

5.1.2. General procedure for the preparation of **5a–d**

Potassium carbonate (2.42 g, 17.5 mmol) and 2,4,5-trichloropyrimidine (1.0 mL, 8.72 mmol) were added to the solution of **4a–d** (8.72 mmol) in DMF (20 mL). The mixture was stirred at room temperature for 2 h. The reaction mixture was poured into ice water and white solid was precipitated. After filtration, filter cake was dried and was used for further steps without purification.

5.1.2.1. 3-(4-((2,5-Dichloropyrimidin-4-yl)oxy)phenyl)propan-1-ol (**5a**). The title compound was obtained starting from **4a**. As a white solid, 98% yield. M.p. 116–118 $^\circ\text{C}$. Analytical data for **5a**: ^1H NMR (300 MHz, CDCl_3): δ 1.88–1.97 (quint, $J = 6.27, 7.14$ Hz, 2H), 2.79–2.74 (t, $J = 7.41$ Hz, 2H), 3.73–3.69 (t, $J = 6.36$ Hz, 2H), 7.08–7.11 (d, $J = 8.49$ Hz, 2H), 7.26–7.29 (d, $J = 8.19$ Hz, 2H), 8.45 (s, 1H); ^{13}C NMR (75 MHz, CDCl_3): δ 165.11, 157.99, 157.38, 149.54, 140.00, 129.54, 120.97, 116.94, 61.86, 33.95, 31.37; ESI-MS: m/z 321.1 $[\text{M} + \text{Na}]^+$; ESI-HRMS (m/z): $[\text{M} + \text{H}]^+$ calcd for $\text{C}_{13}\text{H}_{12}\text{Cl}_2\text{N}_2\text{O}_2$ 299.0349; obsd 299.0374.

5.1.2.2. 2-(4-((2,5-Dichloropyrimidin-4-yl)oxy)phenyl)ethanol (**5b**). The title compound was obtained starting from **4b**. As a white solid, 96% yield. M.p. 179–181 $^\circ\text{C}$. Analytical data for **5b**: ^1H NMR (500 MHz, CDCl_3): δ 2.92 (t, $J = 6.5$ Hz, 2H), 3.91 (t, $J = 6.5$ Hz, 2H), 7.13 (d, $J = 8.4$ Hz, 2H), 7.31 (d, $J = 8.3$ Hz, 2H), 8.46 (s, 1H); ^{13}C NMR (75 MHz, CDCl_3): δ 165.12, 158.11, 157.42, 150.05, 136.94, 130.27, 121.22, 117.00, 63.35, 38.52; ESI-MS: m/z 307.0 $[\text{M} + \text{Na}]^+$; ESI-HRMS (m/z): $[\text{M} + \text{H}]^+$ calcd for $\text{C}_{12}\text{H}_{10}\text{Cl}_2\text{N}_2\text{O}_2$ 285.0192; obsd 285.0211.

5.1.2.3. (4-((2,5-Dichloropyrimidin-4-yl)oxy)phenyl)methanol (5c). The title compound was obtained starting from **4c**. As a white solid, 94% yield. M.p. 107–109 °C. Analytical data for **5c**: ^1H NMR (500 MHz, CDCl_3): δ 4.62 (s, 2H), 7.19 (d, $J = 8.5$ Hz, 2H), 7.47 (d, $J = 8.6$ Hz, 2H), 8.47 (s, 1H); ^{13}C NMR (75 MHz, CDCl_3): δ 165.05, 158.05, 157.42, 150.62, 139.16, 128.18, 121.18, 116.91, 64.20; ESI-MS: m/z 293.0 $[\text{M} + \text{Na}]^+$; ESI-HRMS (m/z): $[\text{M} + \text{H}]^+$ calcd for $\text{C}_{11}\text{H}_8\text{Cl}_2\text{N}_2\text{O}_2$ 271.0036; obsd 271.0051.

5.1.2.4. (3-((2,5-Dichloropyrimidin-4-yl)oxy)phenyl)methanol (5d). The title compound was obtained starting from **4d**. As a white solid, 90% yield. M.p. 139–141 °C. Analytical data for **5d**: ^1H NMR (500 MHz, CDCl_3): δ 4.78 (s, 2H), 7.11 (d, $J = 8.1$ Hz, 1H), 7.21 (s, 1H), 7.30 (d, $J = 7.7$ Hz, 1H), 7.44 (t, $J = 8.0$ Hz, 1H), 8.46 (s, 1H); ^{13}C NMR (75 MHz, CDCl_3): δ 165.12, 158.16, 157.43, 151.71, 143.26, 129.78, 124.62, 120.30, 119.48, 117.02, 64.41; ESI-MS: m/z 293 $[\text{M} + \text{Na}]^+$; ESI-HRMS (m/z): $[\text{M} + \text{H}]^+$ calcd for $\text{C}_{11}\text{H}_8\text{Cl}_2\text{N}_2\text{O}_2$ 271.0036; obsd 271.0051.

5.1.3. 1-(4-(3-Methoxy-4-nitrophenyl)piperazin-1-yl)prop-2-en-1-one (7d)

To a solution of acrylic acid (0.61 g, 8.43 mmol) in anhydrous CH_2Cl_2 (20 mL), dicyclohexylcarbodiimide (DCC) (1.74 g, 8.43 mmol), **7c** (2 g, 8.43 mmol) and 4-dimethylaminopyridine (DMAP) (catalytic amount) were added, and the mixture was stirred at room temperature for 12 h. After filtration, the filtrate was evaporated to dryness in vacuo, and the crude product was purified by column chromatography to obtain **7d** as a yellow solid (89% yield). M.p. 162–163 °C. Analytical data for **7d**: ^1H NMR (500 MHz, CDCl_3): δ 3.45 (t, $J = 5.15$ Hz, 4H), 3.81–3.86 (m, 4H), 3.96 (s, 3H), 5.77 (d, $J = 10.55$ Hz, 1H), 6.35 (s, 1H), 6.37 (d, $J = 16.6$ Hz, 1H), 6.43 (dd, $J = 2.2, 9.3$ Hz, 1H), 6.58 (dd, $J = 10.5, 16.7$ Hz, 1H), 8.00 (d, $J = 9.3$ Hz, 1H); ^{13}C NMR (75 MHz, CDCl_3): δ 164.20, 156.28, 155.54, 144.68, 129.39, 128.91, 123.45, 105.42, 97.02, 55.72, 50.17, 49.78, 44.74, 41.94; ESI-MS: m/z 292.1 $[\text{M} + \text{H}]^+$, 314.1 $[\text{M} + \text{Na}]^+$; ESI-HRMS (m/z): $[\text{M} + \text{H}]^+$ calcd for $\text{C}_{14}\text{H}_{17}\text{N}_3\text{O}_4$ 292.1297, obsd 292.1301.

5.1.4. 1-(4-(4-Amino-3-methoxyphenyl)piperazin-1-yl)prop-2-en-1-one (8c)

Compound **7d** (0.49 g, 1.68 mmol) was dissolved in a mixture of THF (50 mL) and water (50 mL). Iron powder (0.47 g, 8.4 mmol) and ammonium chloride (0.45 g, 8.4 mmol) were then added, and the resulting mixture was heated to 65 °C for 3 h. The reaction mixture was cooled to room temperature and filtered through celite. The THF was removed in vacuo, and the resulting residue was basified with sodium bicarbonate and extracted with ethyl acetate (20 mL) three times. The organic layer was separated and dried using anhydrous sodium sulfate, concentrated, used without further purification. As a yellow oil, 98% yield. Analytical data for **8c**: ^1H NMR (300 MHz, CDCl_3): δ 3.00 (m, 4H), 3.46 (s, 2H), 3.69 (s, 2H), 3.82 (s, 5H), 5.70 (d, $J = 10.5$ Hz, 1H), 6.30 (d, $J = 16.8$ Hz, 1H), 6.39 (d, $J = 8.1$ Hz, 1H), 6.50 (s, 1H), 6.58 (dd, $J = 10.5, 17.1$ Hz, 1H), 6.64 (d, $J = 7.8$ Hz, 1H); ^{13}C NMR (75 MHz, CDCl_3): δ 165.17, 147.80, 144.11, 130.86, 127.71, 127.29, 115.14, 109.97, 102.74, 55.30, 51.75, 51.26, 45.78, 41.94; ESI-MS: m/z 262.2 $[\text{M} + \text{H}]^+$; ESI-HRMS (m/z): $[\text{M} + \text{H}]^+$ calcd for $\text{C}_{14}\text{H}_{19}\text{N}_3\text{O}_2$ 262.1550; obsd 262.1568.

5.1.5. General procedure for the preparation of 9a–h

A flask was charged with compounds **5a–d** (0.70 mmol), **8a–c** (0.70 mmol), TFA (0.08 mL, 1.05 mmol), 2-BuOH (10 mL). The slurry was heated to 100 °C for 3 h. The reaction mixture was allowed to cool to room temperature and, was neutralized with a saturated sodium bicarbonate aqueous solution. The aqueous mixture was then extracted with CH_2Cl_2 (20 mL) three times. The crude product

was purified using flash chromatography with 20:1 (v/v) dichloromethane–methanol to afford compounds **9a–h**.

5.1.5.1. 3-(4-((5-Chloro-2-((2-methoxy-4-(4-methylpiperazin-1-yl)phenyl)amino)pyrimidin-4-yl)oxy)phenyl)propan-1-ol (9a). The title compound was obtained starting from **5a** and **8a**. As a white solid, 81% yield. M.p. 203–204 °C. Analytical data for **9a**: ^1H NMR (500 MHz, CDCl_3): δ 1.98 (quint, $J = 7.2, 6.9$ Hz, 2H), 2.38 (s, 3H), 2.63 (m, 4H), 2.77 (t, $J = 7.7$ Hz, 2H), 3.12 (m, 4H), 3.70 (t, $J = 6.5$ Hz, 2H), 3.81 (s, 3H), 6.19 (d, $J = 6.7$ Hz, 1H), 6.46 (d, $J = 2.0$ Hz, 1H), 7.11 (d, $J = 8.4$ Hz, 2H), 7.27 (d, $J = 8.4$ Hz, 2H), 7.40 (s, 1H), 7.56 (brs, 1H), 8.22 (s, 1H); ^{13}C NMR (75 MHz, DMSO-d_6): δ 163.82, 158.14, 157.77, 151.02, 149.89, 148.29, 139.58, 129.30, 121.59, 120.54, 119.59, 106.24, 103.85, 99.85, 60.06, 55.50, 54.60, 48.56, 45.71, 34.56, 31.04; ESI-MS: m/z 484.3 $[\text{M} + \text{H}]^+$; ESI-HRMS (m/z): $[\text{M} + \text{H}]^+$ calcd for $\text{C}_{25}\text{H}_{30}\text{ClN}_5\text{O}_3$ 484.2110; obsd 484.2124.

5.1.5.2. 2-(4-((5-Chloro-2-((2-methoxy-4-(4-methylpiperazin-1-yl)phenyl)amino)pyrimidin-4-yl)oxy)phenyl)ethanol (9b). The title compound was obtained starting from **5b** and **8a**. As a white solid, 84% yield. M.p. 173–174 °C. Analytical data for **9b**: ^1H NMR (500 MHz, CDCl_3): δ 2.36 (s, 3H), 2.59 (t, $J = 4.5$ Hz, 4H), 2.94 (t, $J = 6.5$ Hz, 2H), 3.11 (t, $J = 4.7$ Hz, 4H), 3.81 (s, 3H), 3.92 (t, $J = 6.5$ Hz, 2H), 6.2 (brs, 1H), 6.45 (d, $J = 2.1$ Hz, 1H), 7.15 (d, $J = 8.4$ Hz, 2H), 7.31 (d, $J = 8.3$ Hz, 2H), 7.41 (s, 1H), 7.59 (brs, 1H), 8.21 (s, 1H); ^{13}C NMR (75 MHz, DMSO-d_6): δ 163.79, 158.18, 157.72, 151.02, 150.13, 148.24, 136.96, 129.91, 122.63, 121.46, 119.60, 106.39, 103.90, 99.85, 62.18, 55.47, 54.59, 48.54, 45.66, 38.36; ESI-MS: m/z 470.3 $[\text{M} + \text{H}]^+$, 504.5 $[\text{M} + \text{Cl}]^-$; ESI-HRMS (m/z): $[\text{M} + \text{H}]^+$ calcd for $\text{C}_{24}\text{H}_{28}\text{ClN}_5\text{O}_3$ 470.1953; obsd 470.1971.

5.1.5.3. (4-((5-Chloro-2-((2-methoxy-4-(4-methylpiperazin-1-yl)phenyl)amino)pyrimidin-4-yl)oxy)phenyl)methanol (9c). The title compound was obtained starting from **5c** and **8a**. As a white solid, 90% yield. M.p. 225–227 °C. Analytical data for **9c**: ^1H NMR (500 MHz, CDCl_3): δ 2.91 (s, 3H), 3.42 (m, 4H), 3.56 (m, 4H), 3.84 (s, 3H), 4.82 (s, 2H), 6.81 (s, 1H), 6.94 (s, 1H), 7.14 (d, $J = 8.2$ Hz, 2H), 7.40 (s, 1H), 7.49 (d, $J = 7.9$ Hz, 2H), 7.78 (brs, 1H), 8.25 (s, 1H); ^{13}C NMR (75 MHz, DMSO-d_6): δ 163.69, 159.18, 158.02, 152.02, 149.13, 148.24, 135.96, 129.91, 122.03, 121.06, 119.20, 106.08, 103.90, 99.85, 62.67, 55.08, 54.59, 48.38, 45.52; ESI-MS: m/z 456.2 $[\text{M} + \text{H}]^+$; ESI-HRMS (m/z): $[\text{M} + \text{H}]^+$ calcd for $\text{C}_{23}\text{H}_{26}\text{ClN}_5\text{O}_3$ 456.1797; obsd 456.1800.

5.1.5.4. 1-(4-((5-Chloro-4-(4-(hydroxymethyl)phenoxy)pyrimidin-2-yl)amino)-3-methoxyphenyl)piperidin-4-ol (9d). The title compound was obtained starting from **5c** and **8b**. As a pale yellow solid, 89% yield. M.p. 207–208 °C. Analytical data for **9d**: ^1H NMR (500 MHz, CDCl_3): δ 1.72 (m, 2H), 2.04 (m, 2H), 2.88 (m, 2H), 3.43 (m, 2H), 3.83 (s, 3H), 3.84 (m, 1H), 4.79 (s, 2H), 6.2 (brs, 1H), 6.47 (d, $J = 2.1$ Hz, 1H), 7.16 (d, $J = 8.4$ Hz, 2H), 7.46 (d, $J = 8.3$ Hz, 3H), 7.59 (brs, 1H), 8.25 (s, 1H); ^{13}C NMR (75 MHz, DMSO-d_6): δ 163.56, 157.99, 157.35, 151.02, 150.13, 148.26, 136.96, 129.87, 122.46, 121.06, 118.98, 106.36, 103.78, 99.81, 67.13, 62.67, 55.08, 47.65, 33.67; ESI-MS: m/z 457.2 $[\text{M} + \text{H}]^+$, 479.2 $[\text{M} + \text{Na}]^+$; ESI-HRMS (m/z): $[\text{M} + \text{H}]^+$ calcd for $\text{C}_{23}\text{H}_{25}\text{ClN}_4\text{O}_4$ 457.1637; obsd 457.1646.

5.1.5.5. 1-(4-(4-((5-Chloro-4-(4-(hydroxymethyl)phenoxy)pyrimidin-2-yl)amino)-3-methoxyphenyl)piperazin-1-yl)prop-2-en-1-one (9e). The title compound was obtained starting from **5c** and **8c**. As a pale yellow solid, 87% yield. M.p. 171–173 °C. Analytical data for **9e**: ^1H NMR (500 MHz, CDCl_3): δ 3.14 (m, 4H), 3.80 (m, 2H), 3.83 (s, 3H), 3.91 (m, 2H), 4.78 (s, 2H), 5.75 (d, $J = 10.6$ Hz, 1H), 6.34 (d, $J = 16.8$ Hz, 2H), 6.56–6.61 (dd, $J = 10.6, 16.8$ Hz, 2H), 7.18 (d, $J = 8.4$ Hz, 2H), 7.47 (d, $J = 8.3$ Hz, 3H), 7.60 (s, 1H), 8.24 (s, 1H); ^{13}C

NMR (75 MHz, DMSO- d_6): δ 164.19, 163.99, 158.48, 157.72, 151.02, 150.13, 148.24, 144.68, 136.96, 129.91, 122.82, 122.23, 121.46, 119.60, 106.41, 103.93, 99.87, 63.49, 55.85, 50.76, 50.33, 45.69, 42.01; ESI-MS: m/z 496.3 [M + H]⁺, 518.3 [M + Na]⁺; ESI-HRMS (m/z): [M + H]⁺ calcd for C₂₅H₂₆ClN₅O₄ 496.1746; obsd 496.1762.

5.1.5.6. (3-((5-Chloro-2-((2-methoxy-4-(4-methylpiperazin-1-yl)phenyl)amino)pyrimidin-4-yl)oxy)phenyl)methanol (**9f**). The title compound was obtained starting from **5d** and **8a**. As a white solid, 92% yield. M.p. 213–215 °C. Analytical data for **9f**: ¹H NMR (500 MHz, CDCl₃): δ 2.88 (s, 3H), 3.14 (m, 2H), 3.46 (m, 2H), 3.51 (m, 2H), 3.58 (m, 2H), 3.82 (s, 3H), 4.72 (s, 2H), 6.32 (d, J = 7.4 Hz, 1H), 6.53 (s, 1H), 7.11 (d, J = 7.7 Hz, 1H), 7.17 (s, 1H), 7.41 (d, J = 7.7 Hz, 1H), 7.46 (t, J = 8.0 Hz, 1H), 7.51 (s, 1H), 7.90 (s, 1H), 8.23 (s, 1H); ¹³C NMR (75 MHz, DMSO- d_6): δ 163.92, 158.42, 157.81, 151.78, 151.23, 147.28, 129.55, 128.12, 127.52, 122.99, 121.03, 120.13, 119.38, 109.01, 103.86, 101.01, 63.26, 55.59, 54.97, 48.86, 45.93; ESI-MS: m/z 456.3 [M + H]⁺; ESI-HRMS (m/z): [M + H]⁺ calcd for C₂₃H₂₆ClN₅O₃ 456.1797; obsd 456.1800.

5.1.5.7. 1-(4-((5-Chloro-4-(3-(hydroxymethyl)phenoxy)pyrimidin-2-yl)amino)-3-methoxyphenyl)piperidin-4-ol (**9g**). The title compound was obtained starting from **5d** and **8b**. As a pale yellow solid, 90% yield. M.p. 183–185 °C. Analytical data for **9g**: ¹H NMR (500 MHz, CDCl₃): δ 1.71 (m, 2H), 2.02 (m, 2H), 2.85 (m, 2H), 3.42 (m, 2H), 3.81 (s, 3H), 3.84 (m, 1H), 4.73 (s, 2H), 6.21 (s, 1H), 6.49 (s, 1H), 7.14 (d, J = 7.7 Hz, 1H), 7.22 (s, 1H), 7.34 (d, J = 7.6 Hz, 1H), 7.42 (s, 1H), 7.46 (t, J = 7.8 Hz, 1H), 7.53 (brs, 1H), 8.22 (s, 1H); ¹³C NMR (75 MHz, DMSO- d_6): δ 163.68, 158.02, 157.39, 152.22, 151.15, 146.98, 129.47, 128.04, 127.52, 122.98, 121.09, 120.04, 119.40, 108.59, 104.87, 99.98, 66.98, 62.77, 55.45, 48.73, 33.80; ESI-MS: m/z 457.2 [M + H]⁺, 479.2 [M + Na]⁺; ESI-HRMS (m/z): [M + H]⁺ calcd for C₂₃H₂₅ClN₄O₄ 457.1637; obsd 457.1646.

5.1.5.8. 1-(4-(4-((5-Chloro-4-(3-(hydroxymethyl)phenoxy)pyrimidin-2-yl)amino)-3-methoxyphenyl)piperazin-1-yl)prop-2-en-1-one (**9h**). The title compound was obtained starting from **5d** and **8c**. As a pale yellow solid, 85% yield. M.p. 178–180 °C. Analytical data for **9h**: ¹H NMR (500 MHz, CDCl₃): δ 3.11 (m, 4H), 3.77 (m, 2H), 3.83 (s, 3H), 3.89 (m, 2H), 4.74 (s, 2H), 5.75 (dd, J = 1.8, 10.6 Hz, 1H), 6.27 (s, 1H), 6.33 (dd, J = 1.7, 16.8 Hz, 1H), 6.54 (s, 1H), 6.59 (dd, J = 10.6, 16.8 Hz, 1H), 7.14 (d, J = 7.8 Hz, 1H), 7.22 (s, 1H), 7.35 (d, J = 7.6 Hz, 1H), 7.46 (t, J = 7.8 Hz, 1H), 7.52 (s, 1H), 7.60 (s, 1H), 8.24 (s, 1H); ¹³C NMR (75 MHz, DMSO- d_6): δ 164.18, 163.72, 158.12, 157.71, 151.90, 151.15, 147.18, 144.68, 129.25, 128.04, 127.52, 123.45, 122.74, 120.84, 119.94, 119.40, 107.59, 104.26, 100.93, 62.27, 55.58, 50.01, 49.39, 44.64, 41.06; ESI-MS: m/z 496.3 [M + H]⁺, 518.3 [M + Na]⁺; ESI-HRMS (m/z): [M + H]⁺ calcd for C₂₅H₂₆ClN₅O₄ 496.1746; obsd 496.1762.

5.1.6. General procedure for the preparation of **10a–h**

Compounds **9a–h** (0.34 mmol) were dissolved in 10 mL of anhydrous THF, to which 65% NaH (25 mg, 0.68 mmol) was slowly added under stirring at 0 °C. Subsequently, 3,4-bis(phenylsulfonyl)-1,2,5-oxadiazole-2-oxide (**11**) (249 mg, 0.68 mmol) was added, and the obtained mixture was allowed to stir for 0.5 h at room temperature. 15 mL of H₂O was added to the mixture. The organic layer was separated, then the water layer was extracted with CH₂Cl₂ (10 mL × 2). The combined organic layer was washed with water and brine, dried over anhydrous Na₂SO₄, and concentrated in vacuo. The crude product was purified by column chromatography (MeOH/CH₂Cl₂ 1:25 v/v) to give the title compounds.

5.1.6.1. 4-(3-(4-((5-Chloro-2-((2-methoxy-4-(4-methylpiperazin-1-yl)phenyl)amino)pyrimidin-4-yl)oxy)phenyl)propoxy)-3-

(phenylsulfonyl)-1,2,5-oxadiazole-2-oxide (**10a**). The title compound was obtained starting from **9a**. As a yellow solid, 55% yield. M.p. 77–79 °C. Analytical data for **10a**: ¹H NMR (300 MHz, CDCl₃): δ 2.26 (m, 2H), 2.45 (s, 3H), 2.77 (m, 4H), 2.91 (t, J = 6.8 Hz, 2H), 3.18 (m, 4H), 3.82 (s, 3H), 4.49 (t, J = 5.6 Hz, 2H), 6.18 (d, J = 8.3 Hz, 1H), 6.46 (d, J = 2.1 Hz, 1H), 7.15 (d, J = 8.4 Hz, 2H), 7.31 (d, J = 8.3 Hz, 2H), 7.52–7.55 (brs, 1H), 7.63 (t, J = 7.9 Hz, 2H), 7.73–7.79 (t, J = 7.3 Hz, 2H), 8.09 (d, J = 7.5 Hz, 2H), 8.24 (s, 1H); ¹³C NMR (75 MHz, CDCl₃): δ 164.02, 158.37, 157.12, 157.01, 150.44, 148.29, 146.61, 137.58, 137.30, 135.19, 129.22, 128.95, 128.02, 121.80, 121.54, 118.68, 110.07, 107.66, 100.14, 69.90, 55.14, 54.30, 49.05, 44.96, 30.61, 29.70; ESI-MS: m/z 708.0 [M + H]⁺; ESI-HRMS (m/z): [M + H]⁺ calcd for C₃₃H₃₄ClN₇O₇S 708.2007; obsd 708.2014.

5.1.6.2. 4-(4-((5-Chloro-2-((2-methoxy-4-(4-methylpiperazin-1-yl)phenyl)amino)pyrimidin-4-yl)oxy)phenyl)ethoxy)-3-(phenylsulfonyl)-1,2,5-oxadiazole-2-oxide (**10b**). The title compound was obtained starting from **9b**. As a yellow solid, 67% yield. M.p. 88–90 °C. Analytical data for **10b**: ¹H NMR (300 MHz, CDCl₃): δ 2.37 (s, 3H), 2.61 (m, 4H), 3.10 (m, 4H), 3.27 (t, J = 6.6 Hz, 2H), 3.79 (s, 3H), 4.68 (t, J = 6.6 Hz, 2H), 6.18 (d, J = 7.2 Hz, 1H), 6.44 (d, J = 1.5 Hz, 1H), 7.21 (d, J = 8.4 Hz, 2H), 7.41 (d, J = 8.1 Hz, 3H), 7.54 (t, J = 4.8 Hz, 2H), 7.69 (d, J = 7.5 Hz, 2H), 7.93 (d, J = 7.8 Hz, 2H), 8.25 (s, 1H); ¹³C NMR (75 MHz, CDCl₃): δ 163.95, 158.36, 157.22, 157.01, 151.02, 148.30, 146.70, 137.50, 135.12, 133.51, 129.71, 129.19, 127.88, 127.28, 121.89, 121.40, 118.75, 109.88, 107.26, 99.88, 71.05, 55.07, 54.57, 49.49, 45.52, 33.86; ESI-MS: m/z 694.3 [M + H]⁺; ESI-HRMS (m/z): [M + H]⁺ calcd for C₃₂H₃₂ClN₇O₇S 694.1851; obsd 694.1858.

5.1.6.3. 4-((4-((5-Chloro-2-((2-methoxy-4-(4-methylpiperazin-1-yl)phenyl)amino)pyrimidin-4-yl)oxy)benzyl)oxy)-3-(phenylsulfonyl)-1,2,5-oxadiazole-2-oxide (**10c**). The title compound was obtained starting from **9c**. As a yellow solid, 87% yield. M.p. 195–197 °C. Analytical data for **10c**: ¹H NMR (300 MHz, CDCl₃): δ 2.34 (s, 3H), 2.56 (t, J = 4.8 Hz, 4H), 3.11 (t, J = 4.62 Hz, 4H), 3.81 (s, 3H), 5.52 (s, 2H), 6.26 (d, J = 8.79 Hz, 1H), 6.47 (d, J = 2.31 Hz, 1H), 7.29 (d, J = 8.49 Hz, 2H), 7.40 (s, 1H), 7.52–7.60 (m, 4H), 7.73 (m, 2H), 8.04 (d, J = 7.41 Hz, 2H), 8.29 (s, 1H); ¹³C NMR (75 MHz, CDCl₃): δ 163.68, 159.51, 158.15, 157.33, 157.03, 152.48, 148.33, 146.82, 137.47, 135.17, 130.61, 129.19, 128.90, 128.07, 122.04, 121.01, 118.87, 110.07, 107.40, 99.71, 71.54, 55.10, 54.55, 49.38, 45.52; ESI-MS: m/z 680.1 [M + H]⁺; ESI-HRMS (m/z): [M + H]⁺ calcd for C₃₁H₃₀ClN₇O₇S 680.1694; obsd 680.1706.

5.1.6.4. 4-(4-((5-Chloro-2-((4-(4-hydroxypiperidin-1-yl)-2-methoxyphenyl)amino)pyrimidin-4-yl)oxy)benzyl)-3-(phenylsulfonyl)-1,2,5-oxadiazole-2-oxide (**10d**). The title compound was obtained starting from **9d**. As a yellow solid, 82% yield. M.p. 155–157 °C. Analytical data for **10d**: ¹H NMR (300 MHz, CDCl₃): δ 1.68 (q, J = 9 Hz, 2H), 1.99 (q, J = 9.4 Hz, 2H), 2.84 (t, J = 8.1 Hz, 2H), 3.43 (t, J = 6.5 Hz, 2H), 3.81 (s, 4H), 5.52 (s, 2H), 6.27 (d, J = 8.79 Hz, 1H), 6.50 (d, J = 2.31 Hz, 1H), 7.29 (d, J = 8.49 Hz, 2H), 7.43 (s, 1H), 7.52–7.62 (m, 4H), 7.73 (m, 2H), 8.04 (d, J = 7.41 Hz, 2H), 8.26 (s, 1H); ¹³C NMR (75 MHz, CDCl₃): δ 157.35, 157.03, 152.51, 148.26, 146.92, 135.16, 130.60, 129.18, 128.88, 128.08, 122.06, 120.94, 118.78, 107.84, 100.44, 71.54, 67.13, 55.09, 47.72, 33.77; ESI-MS: m/z 681.4 [M + H]⁺; ESI-HRMS (m/z): [M + Na]⁺ calcd for C₃₁H₂₉ClN₆O₈S 703.1354; obsd 703.1361.

5.1.6.5. 4-(4-((2-((4-(4-Acryloylpiperazin-1-yl)-2-methoxyphenyl)amino)-5-chloropyrimidin-4-yl)oxy)benzyl)-3-(phenylsulfonyl)-1,2,5-oxadiazole-2-oxide (**10e**). The title compound was obtained starting from **9e**. As a yellow solid, 83% yield. M.p. 162–164 °C. Analytical data for **10e**: ¹H NMR (300 MHz, CDCl₃): δ 3.08 (m, 4H), 3.71 (brs, 2H), 3.83 (s, 5H), 5.53 (s, 2H), 5.73 (d, J = 10.32 Hz, 1H),

6.32 (d, $J = 16.77$ Hz, 2H), 6.49 (brs, 1H), 6.59 (dd, $J = 10.5, 10.8$ Hz, 1H), 7.31 (d, $J = 8.13$ Hz, 2H), 7.48 (s, 1H), 7.55 (d, $J = 8.16$ Hz, 2H), 7.60 (d, $J = 7.59$ Hz, 2H), 7.75 (t, $J = 7.17$ Hz, 2H), 8.04 (d, $J = 7.86$ Hz, 2H), 8.28 (s, 1H); ^{13}C NMR (75 MHz, CDCl_3): δ 165.31, 164.34, 158.47, 157.87, 157.47, 152.99, 148.71, 147.96, 146.85, 138.23, 135.70, 131.13, 129.70, 129.39, 128.58, 128.11, 127.32, 122.52, 119.07, 108.56, 100.88, 72.05, 55.65, 50.72, 50.33, 45.75, 41.93; ESI-MS: m/z 720.1 $[\text{M} + \text{H}]^+$; ESI-HRMS (m/z): $[\text{M} + \text{H}]^+$ calcd for $\text{C}_{33}\text{H}_{30}\text{ClN}_7\text{O}_8\text{S}$ 720.1643; obsd 720.1655.

5.1.6.6. 4-((3-((5-Chloro-2-((2-methoxy-4-(4-methylpiperazin-1-yl)phenyl)amino)pyrimidin-4-yl)oxy)benzyl)oxy)-3-(phenylsulfonyl)-1,2,5-oxadiazole-2-oxide (**10f**). The title compound was obtained starting from **9f**. As a yellow solid, 90% yield. M.p. 206–208 °C. Analytical data for **10f**: ^1H NMR (300 MHz, CDCl_3), δ : 2.39 (s, 3H), 2.63 (m, 4H), 3.13 (m, 4H), 3.81 (s, 3H), 5.48 (s, 2H), 6.16 (d, $J = 8.1$ Hz, 1H), 6.45 (d, $J = 1.89$ Hz, 1H), 7.28 (s, 2H), 7.43 (d, $J = 7.2$ Hz, 2H), 7.53 (t, $J = 7.83$ Hz, 4H), 7.70 (t, $J = 7.5$ Hz, 1H), 7.99 (d, $J = 7.8$ Hz, 2H), 8.25 (s, 1H); ^{13}C NMR (75 MHz, CDCl_3): δ 164.31, 163.91, 158.50, 157.88, 157.51, 152.73, 148.81, 147.28, 137.85, 135.61, 135.51, 129.93, 129.63, 128.50, 125.22, 123.02, 121.75, 121.48, 119.25, 107.74, 100.17, 71.82, 55.59, 55.07, 49.86, 46.03; ESI-MS: m/z 680.1 $[\text{M} + \text{H}]^+$; ESI-HRMS (m/z): $[\text{M} + \text{H}]^+$ calcd for $\text{C}_{31}\text{H}_{30}\text{ClN}_7\text{O}_7\text{S}$ 680.1694; obsd 680.1706.

5.1.6.7. 4-((3-((5-Chloro-2-((4-(4-hydroxypiperidin-1-yl)-2-methoxyphenyl)amino)pyrimidin-4-yl)oxy)benzyl)oxy)-3-(phenylsulfonyl)-1,2,5-oxadiazole-2-oxide (**10g**). The title compound was obtained starting from **9g**. As a yellow solid, 85% yield. M.p. 86–88 °C. Analytical data for **10g**: ^1H NMR (300 MHz, CDCl_3), δ : 1.68 (q, $J = 9$ Hz, 2H), 1.99 (q, $J = 9.4$ Hz, 2H), 2.82 (t, $J = 8.1$ Hz, 2H), 3.39 (t, $J = 6.5$ Hz, 2H), 3.81 (s, 4H), 5.48 (s, 2H), 6.16 (brs, 1H), 6.48 (d, $J = 1.89$ Hz, 1H), 7.28 (s, 2H), 7.43 (d, $J = 7.2$ Hz, 2H), 7.53 (t, $J = 7.83$ Hz, 4H), 7.70 (t, $J = 7.5$ Hz, 1H), 7.99 (d, $J = 7.8$ Hz, 2H), 8.26 (s, 1H); ^{13}C NMR (75 MHz, CDCl_3): δ 158.01, 157.39, 156.97, 152.22, 148.26, 146.98, 137.48, 135.12, 135.00, 129.45, 129.13, 128.02, 124.72, 122.56, 121.28, 120.91, 107.71, 100.39, 71.33, 67.17, 55.10, 47.73, 33.78; ESI-MS: m/z 681.2 $[\text{M} + \text{H}]^+$; ESI-HRMS (m/z): $[\text{M} + \text{Na}]^+$ calcd for $\text{C}_{31}\text{H}_{29}\text{ClN}_6\text{O}_8\text{S}$ 703.1354; obsd 703.1361.

5.1.6.8. 4-((3-((2-((4-(4-Acryloylpiperazin-1-yl)-2-methoxyphenyl)amino)-5-chloropyrimidin-4-yl)oxy)benzyl)oxy)-3-(phenylsulfonyl)-1,2,5-oxadiazole-2-oxide (**10h**). The title compound was obtained starting from **9h**. As a yellow solid, 81% yield. M.p. 160–162 °C. Analytical data for **10h**: ^1H NMR (300 MHz, CDCl_3), δ : 3.06 (brs, 4H), 3.70 (brs, 2H), 3.82 (s, 5H), 5.48 (s, 2H), 5.72 (d, $J = 10.44$ Hz, 1H), 6.15 (brs, 1H), 6.32 (d, $J = 16.74$ Hz, 1H), 6.46 (s, 1H), 6.60 (dd, $J = 10.5, 10.47$ Hz, 1H), 7.26 (s, 2H), 7.44 (d, $J = 7.5$ Hz, 1H), 7.53 (t, $J = 7.41$ Hz, 5H), 7.69 (t, $J = 7.26$ Hz, 1H), 7.98 (d, $J = 7.86$ Hz, 2H), 8.27 (s, 1H); ^{13}C NMR (75 MHz, CDCl_3): δ 165.36, 164.38, 158.50, 157.90, 157.40, 152.75, 148.70, 146.78, 137.96, 135.64, 135.56, 129.96, 129.64, 128.49, 128.09, 127.34, 125.28, 123.06, 122.32, 121.80, 118.96, 108.36, 100.84, 71.83, 55.66, 50.72, 50.33, 45.75, 41.90; ESI-MS: m/z 720.1 $[\text{M} + \text{H}]^+$; ESI-HRMS (m/z): $[\text{M} + \text{H}]^+$ calcd for $\text{C}_{33}\text{H}_{30}\text{ClN}_7\text{O}_8\text{S}$ 720.1643; obsd 720.1655.

5.2. Biological assays

5.2.1. Cell lines and reagents

H1975 (NSCLC, EGFR L858R/T790M), HCC827 (NSCLC, EGFR del E746_A750), A431 (epidermoid carcinoma, EGFR overexpression), A549 (NSCLC, EGFR wild type), 16HBE (human bronchial epithelial) cells were obtained from ATCC. The cells were maintained at 37 °C in a 5% CO_2 incubator in DMEM or RPMI 1640 (Hyclone) containing 10% fetal bovine serum (FBS, Biochrom, AG).

5.2.2. In vitro enzymatic activity assay

Wild type (WT) and EGFR mutants (L858R, L858R/T790M) and the Z'-Lyte Kinase Kit were purchased from Invitrogen. The experiments were performed according to the instructions of the manufacturer. Briefly, the concentrations of different kinases were determined by optimization experiments and the respective concentration was: EGFR (PV3872, Invitrogen) 0.287 $\mu\text{g}/\mu\text{L}$, EGFR-L858R (PV4128, Invitrogen) 0.054 $\mu\text{g}/\mu\text{L}$, EGFR-L858R/T790M (PV4879, Invitrogen) 0.055 $\mu\text{g}/\mu\text{L}$. Ten concentration gradients were set for all the tested compounds from 5.1×10^{-9} M to 1×10^{-4} M in DMSO; a 4 \times compound solution was prepared. An ATP solution in 1.33 \times Kinase Buffer, and a Kinase/Peptide Mixture containing 2 \times kinase and Tyr 4 peptide were prepared right before use. The 10 μL Kinase Reactions were consisted of 2.5 μL compound solution, 5 μL Kinase/Peptide Mixture, and 2.5 μL ATP solution. 5 μL phospho-peptide solution instead of Kinase/Peptide Mixture was used as 100% phosphorylation control. 2.5 μL 1.33 \times Kinase Buffer instead of ATP solution was used as 100% inhibition control, while 2.5 μL 4% DMSO instead of compound solution was used as 0% inhibition control. Mixed the plate thoroughly and incubated for 1 h at 25 °C. 5 μL Development Solution was added to each well and the plate was incubated for 1 h at 25 °C; the non-phospho-peptides were cleaved in this time. In the end, 5 μL Stop Reagent was added to stop reaction. Plate was measured on EnVision Multilabel Reader (Perkin–Elmer). Curve fitting and data presentations were performed using Graph Pad Prism version 5.0. Every experiment was repeated at least 3 times.

5.2.3. MTT assay

1000 cells/well of H1975, 2000 cells/well of HCC827, A431, A549 and 16HBE were cultured in 8% FBS respective growth medium in 96-well microplates overnight. The cells were then treated in triplicate with various concentrations of each compound and cultured in 5% FBS medium for 72 h. Control cells were treated with vehicle alone. During the last 4 h of incubation, the cells were exposed to tetrazolium dye (MTT) solution (5 mg/mL, 20 μL /well). The generated formazan crystals were dissolved in 100 μL of dimethyl sulfoxide (DMSO), and the absorbance was read spectrophotometrically at 570 nm using an enzyme-linked immunosorbent assay plate reader. The data were calculated using Graph Pad Prism version 5.0. The IC_{50} s were fitted using a non-linear regression model with a sigmoidal dose response.

5.2.4. Nitrite measurement in vitro

The levels of nitrite produced by individual compounds in the cells were determined by the colorimetric assay using the nitrite colorimetric assay kit (Beyotime, China), according to the manufacturer's instructions. Briefly, H1975 or 16HBE cells (1×10^6 /well) were treated with 100 μM of each compound for 150 min. Subsequently, the cells were harvested and their cell lysates were prepared, then mixing with Griess for 10 min, followed by measuring at 540 nm. The cells treated with DMSO were used as negative controls for the background levels of nitrite production, while sodium nitrite at different concentrations was used as the positive control for the standard curve.

5.2.5. Western blotting analysis

The H1975 cells were incubated with 0.01, 0.1 or 1 μM WZ4002, **10h** or vehicle control (0.1%DMSO) for 6 h. Following incubation, the cells were harvested and lysed. The cell lysates (50 $\mu\text{g}/\text{lane}$) were separated by sodium dodecyl sulfate-polyacrylamide gel electrophoresis (7.5% gel) and transferred onto nitrocellulose membranes. After they were blocked with 5% fat-free milk, the target proteins were probed with anti-EGFR, antiphospho-EGFR (Tyr1068), anti-AKT, antiphospho-AKT (Ser473), anti-ERK, antiphospho-ERK (Thr202/

Tyr204), and anti- β -actin antibodies (Cell Signaling, Boston, MA), respectively. The bound antibodies were detected by horseradish peroxidase (HRP)-conjugated second antibodies and visualized using the enhanced chemiluminescent reagent.

Acknowledgements

The work was financially supported by the Fundamental Research Funds for the Central Universities (NO. JKY2011021) and the Innovative Program for Postgraduate Students of Jiangsu province (NO. ZJ11317).

Appendix A. Supplementary data

Supplementary data related to this article can be found at <http://dx.doi.org/10.1016/j.ejmech.2013.05.026>.

References

- [1] R. Siegel, D. Naishadham, A. Jemal, Cancer statistics, 2013, *CA Cancer J. Clin.* 63 (2013) 11–30.
- [2] A.G. Pallis, L. Serfass, R. Dziadziusko, J.P. van Meerbeeck, D. Fennell, D. Lacombe, J. Welch, C. Gridelli, Targeted therapies in the treatment of advanced/metastatic NSCLC, *Eur. J. Cancer* 45 (2009) 2473–2487.
- [3] K. Gately, J. O'Flaherty, F. Cappuzzo, R. Pirker, K. Kerr, K. O'Byrne, The role of the molecular footprint of EGFR in tailoring treatment decisions in NSCLC, *J. Clin. Pathol.* 65 (2012) 1–7.
- [4] M.A. Olayioye, R.M. Neve, H.A. Lane, N.E. Hynes, The ErbB signaling network: receptor heterodimerization in development and cancer, *Embo. J.* 19 (2000) 3159–3167.
- [5] J. Mendelsohn, J. Baselga, Epidermal growth factor receptor targeting in cancer, *Semin. Oncol.* 33 (2006) 369–385.
- [6] M. Ladanyi, W. Pao, Lung adenocarcinoma: guiding EGFR-targeted therapy and beyond, *Mod. Pathol.* 21 (Suppl. 2) (2008) S16–S22.
- [7] S. Kobayashi, T.J. Boggon, T. Dayaram, P.A. Janne, O. Kocher, M. Meyerson, B.E. Johnson, M.J. Eck, D.G. Tenen, B. Halmos, EGFR mutation and resistance of non-small-cell lung cancer to gefitinib, *New Engl. J. Med.* 352 (2005) 786–792.
- [8] W. Pao, V.A. Miller, K.A. Politi, G.J. Riely, R. Somwar, M.F. Zakowski, M.G. Kris, H. Varmus, Acquired resistance of lung adenocarcinomas to gefitinib or erlotinib is associated with a second mutation in the EGFR kinase domain, *PLoS Med.* 2 (2005) 225–235.
- [9] C.H. Yun, K.E. Mengwasser, A.V. Toms, M.S. Woo, H. Greulich, K.K. Wong, M. Meyerson, M.J. Eck, The T790M mutation in EGFR kinase causes drug resistance by increasing the affinity for ATP, *Proc. Natl. Acad. Sci. U. S. A.* 105 (2008) 2070–2075.
- [10] P.A. Janne, J. von Pawel, R.B. Cohen, L. Crino, C.A. Butts, S.S. Olson, I.A. Eisenman, A.A. Chiappori, B.Y. Yeap, P.F. Lenehan, K. Dasse, M. Sheeran, P.D. Bonomi, Multicenter, randomized, phase II trial of CI-1033, an irreversible pan-ERBB inhibitor, for previously treated advanced non small-cell lung cancer, *J. Clin. Oncol.* 25 (2007) 3936–3944.
- [11] F.A. Eskens, C.H. Mom, A.S. Planting, J.A. Gietema, A. Amelsberg, H. Huisman, L. van Doorn, H. Burger, P. Stopfer, J. Verweij, E.G. de Vries, A phase I dose escalation study of BIBW 2992, an irreversible dual inhibitor of epidermal growth factor receptor 1 (EGFR) and 2 (HER2) tyrosine kinase in a 2-week on, 2-week off schedule in patients with advanced solid tumours, *Br. J. Cancer* 98 (2008) 80–85.
- [12] S.K. Rabindran, C.M. Discafani, E.C. Rosfjord, M. Baxter, M.B. Floyd, J. Golas, W.A. Hallett, B.D. Johnson, R. Nilakantan, E. Overbeek, M.F. Reich, R. Shen, X. Shi, H.R. Tsou, Y.F. Wang, A. Wissner, Antitumor activity of HKI-272, an orally active, irreversible inhibitor of the HER-2 tyrosine kinase, *Cancer Res.* 64 (2004) 3958–3965.
- [13] J.A. Engelman, K. Zejnullahu, C.M. Gale, E. Lifshits, A.J. Gonzales, T. Shimamura, F. Zhao, P.W. Vincent, G.N. Naumov, J.E. Bradner, I.W. Althaus, L. Gandhi, G.I. Shapiro, J.M. Nelson, J.V. Heymach, M. Meyerson, K.K. Wong, P.A. Janne, PF00299804, an irreversible pan-ERBB inhibitor, is effective in lung cancer models with EGFR and ERBB2 mutations that are resistant to gefitinib, *Cancer Res.* 67 (2007) 11924–11932.
- [14] G.J. Riely, Second-generation epidermal growth factor receptor tyrosine kinase inhibitors in non-small cell lung cancer, *J. Thorac. Oncol.* 3 (2008) S146–S149.
- [15] D.W. Fry, A.J. Bridges, W.A. Denny, A. Doherty, K.D. Greis, J.L. Hicks, K.E. Hook, P.R. Keller, W.R. Leopold, J.A. Loo, D.J. McNamara, J.M. Nelson, V. Sherwood, J.B. Smaill, S. Trumpp-Kallmeyer, E.M. Dobrusin, Specific, irreversible inactivation of the epidermal growth factor receptor and erbB2, by a new class of tyrosine kinase inhibitor, *Proc. Natl. Acad. Sci. U. S. A.* 95 (1998) 12022–12027.
- [16] C. Carmi, A. Lodola, S. Rivara, F. Vacondio, A. Cavazzoni, R.R. Alfieri, A. Ardizzoni, P.G. Petronini, M. Mor, Epidermal growth factor receptor irreversible inhibitors: chemical exploration of the cysteine-trap portion, *Mini. Rev. Med. Chem.* 11 (2011) 1019–1030.
- [17] L.V. Sequist, B. Besse, T.J. Lynch, V.A. Miller, K.K. Wong, B. Gitlitz, K. Eaton, C. Zacharchuk, A. Freyman, C. Powell, R. Ananthkrishnan, S. Quinn, J.C. Soria, Neratinib, an irreversible pan-ErbB receptor tyrosine kinase inhibitor: results of a phase II trial in patients with advanced non-small-cell lung cancer, *J. Clin. Oncol.* 28 (2010) 3076–3083.
- [18] W.J. Zhou, D. Ercan, P.A. Janne, N.S. Gray, Discovery of selective irreversible inhibitors for EGFR-T790M, *Bioorg. Med. Chem. Lett.* 21 (2011) 638–643.
- [19] W. Zhou, D. Ercan, L. Chen, C.H. Yun, D. Li, M. Capelletti, A.B. Cortot, L. Chiriac, R.E. Jacob, R. Padera, J.R. Engen, K.K. Wong, M.J. Eck, N.S. Gray, P.A. Janne, Novel mutant-selective EGFR kinase inhibitors against EGFR T790M, *Nature* 462 (2009) 1070–1074.
- [20] D. Fukumura, S. Kashiwagi, R.K. Jain, The role of nitric oxide in tumour progression, *Nat. Rev. Cancer* 6 (2006) 521–534.
- [21] B. Bonavida, S. Baritaki, S. Huerta-Yepez, M.I. Vega, D. Chatterjee, K. Yeung, Novel therapeutic applications of nitric oxide donors in cancer: roles in chemo- and immunosensitization to apoptosis and inhibition of metastases, *Nitric Oxide* 19 (2008) 152–157.
- [22] N.P. Konovalova, S.A. Goncharova, L.M. Volkova, T.A. Rajewskaya, L.T. Eremenko, A.M. Korolev, Nitric oxide donor increases the efficiency of cytostatic therapy and retards the development of drug resistance, *Nitric Oxide* 8 (2003) 59–64.
- [23] G. Aguirre, M. Boiani, H. Cerecetto, M. Fernandez, M. Gonzalez, E. Leon, C. Pintos, S. Raymondo, C. Arredondo, J.P. Pacheco, M.A. Basombrio, Furoxan derivatives as cytotoxic agents: preliminary in vivo antitumoral activity studies, *Pharmazie* 61 (2006) 54–59.
- [24] L. Chen, Y. Zhang, X. Kong, E. Lan, Z. Huang, S. Peng, D.L. Kaufman, J. Tian, Design, synthesis, and antihepatocellular carcinoma activity of nitric oxide releasing derivatives of oleanolic acid, *J. Med. Chem.* 51 (2008) 4834–4838.
- [25] Z. Huang, Y. Zhang, L. Zhao, Y. Jing, Y. Lai, L. Zhang, Q. Guo, S. Yuan, J. Zhang, L. Chen, S. Peng, J. Tian, Synthesis and anti-human hepatocellular carcinoma activity of new nitric oxide-releasing glycosyl derivatives of oleanolic acid, *Org. Biomol. Chem.* 8 (2010) 632–639.
- [26] Y. Ling, X. Ye, Z. Zhang, Y. Zhang, Y. Lai, H. Ji, S. Peng, J. Tian, Novel nitric oxide-releasing derivatives of farnesylthiosalicylic acid: synthesis and evaluation of antihepatocellular carcinoma activity, *J. Med. Chem.* 54 (2011) 3251–3259.
- [27] X. Wang, X. Li, J. Xue, Y. Zhao, Y. Zhang, A novel and efficient procedure for the preparation of allylic alcohols from α,β -unsaturated carboxylic esters using $\text{LiAlH}_4/\text{BnCl}$, *Tetrahedron Lett.* 50 (2009) 413–415.
- [28] S. Chang, L. Zhang, S. Xu, J. Luo, X. Lu, Z. Zhang, T. Xu, Y. Liu, Z. Tu, Y. Xu, X. Ren, M. Geng, J. Ding, D. Pei, K. Ding, Design, synthesis, and biological evaluation of novel conformationally constrained inhibitors targeting epidermal growth factor receptor threonine⁷⁹⁰ \rightarrow methionine⁷⁹⁰ mutant, *J. Med. Chem.* 55 (2012) 2711–2723.
- [29] E.A. Jares-Erijman, T.M. Jovin, FRET imaging, *Nat. Biotechnol.* 21 (2003) 1387–1395.
- [30] P.N. Coneski, M.H. Schoenfish, Nitric oxide release: part III. Measurement and reporting, *Chem. Soc. Rev.* 41 (2012) 3753–3758.
- [31] M. Feelisch, K. Schonafinger, E. Noack, Thiol-mediated generation of nitric oxide accounts for the vasodilator action of furoxans, *Biochem. Pharmacol.* 44 (1992) 1149–1157.
- [32] H. Cerecetto, W. Porcal, Pharmacological properties of furoxans and benzo-furoxans: recent developments, *Mini. Rev. Med. Chem.* 5 (2005) 57–71.
- [33] N.S. Gray, W. Zhou, Preparation of EGFR Modulators for Treating or Preventing Kinase-mediated Disorders, *PCT Int. Appl. WO* 2011/079231, 2011.
- [34] K. Kuntz, D.E. Uehling, A.G. Waterson, K.A. Emmitte, K. Stevens, J.B. Shotwell, S.C. Smith, K.E. Nailor, J.M. Salovich, B.J. Wilson, M. Cheung, R.A. Mook, E.W. Baum, G. Moorthy, Preparation of Imidazopyridines as Inhibitors of IGF-1R and IR and One or Both of EGFR and ErbB2 Kinases for Treating Neoplasm, *U.S. Pat. Appl. Publ. US* 20080300242, 2008.
- [35] N. Kwiatkowski, N. Jelluma, P. Filippakopoulos, M. Soundararajan, M.S. Manak, M. Kwon, H.G. Choi, T. Sim, Q.L. Deveraux, S. Rottmann, D. Pellman, J.V. Shah, G.J. Kops, S. Knapp, N.S. Gray, Small-molecule kinase inhibitors provide insight into Mps1 cell cycle function, *Nat. Chem. Biol.* 6 (2010) 359–368.